

On Bernoulli's free boundary problem with a random boundary

M. Dambrine, H. Harbrecht, M. D. Peters, B. Puig

Departement Mathematik und Informatik
Fachbereich Mathematik
Universität Basel
CH-4051 Basel

Preprint No. 2016-31
December 2016

www.math.unibas.ch

ON BERNOULLI'S FREE BOUNDARY PROBLEM WITH A RANDOM BOUNDARY

M. DAMBRINE, H. HARBRECHT, M. D. PETERS, AND B. PUIG

ABSTRACT. This article is dedicated to the solution of Bernoulli's exterior free boundary problem in the situation of a random interior boundary. We describe two different frameworks to define the expectation and the deviation of the resulting annular domain. In order to compare these approaches, we present analytical examples for the case of a circular interior boundary. Additionally, numerical experiments are performed for more general geometric configurations. For the numerical approximation of the expectation and the deviation, we propose a sampling method like the Monte Carlo or the quasi-Monte Carlo quadrature. Each particular realization of the free boundary is then computed by the trial method, which is a fixed-point like iteration for the solution of Bernoulli's free boundary problem.

1. INTRODUCTION

In the past, much attention has been given to the numerical solution of free boundary problems, see e.g. [6, 5, 11, 18, 21, 26] and the references therein. As a consequence, there are nowadays various efficient methods in order to perform the actual computations. In particular, studying the influence of uncertainties of the input parameters of such problems is now possible. In this article, we consider the case of Bernoulli's exterior problem when the input data –here the interior boundary– is random.

Let us briefly recall the situation of the original problem. To that end, let $T \subset \mathbb{R}^n$ denote a bounded domain with boundary $\partial T = \Gamma$. Inside the domain T we assume the existence of a simply connected subdomain $S \subset T$ with boundary $\partial S = \Sigma$. The resulting annular domain $T \setminus \bar{S}$ is denoted by D . The topological situation is visualized in Figure 1.1.

Key words and phrases. Bernoulli's free boundary problem, random boundary.

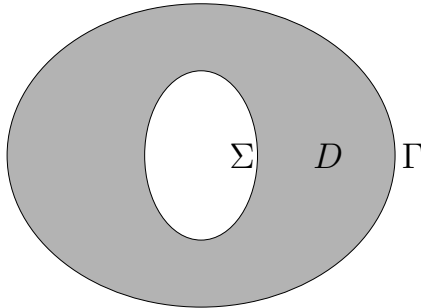


FIGURE 1.1. The domain D and its boundaries Γ and Σ .

We aim at solving the subsequent overdetermined boundary value problem in the annular domain D

$$(1.1) \quad \begin{cases} \Delta u = 0 & \text{in } D, \\ \|\nabla u\| = f & \text{on } \Gamma, \\ u = 0 & \text{on } \Gamma, \\ u = 1 & \text{on } \Sigma. \end{cases}$$

where $f > 0$ is a given constant. The non-negativity of the Dirichlet data implies that u is positive in D . Hence, there holds the identity

$$\|\nabla u\| \equiv -\frac{\partial u}{\partial \mathbf{n}} \quad \text{on } \Gamma,$$

since u admits homogeneous Dirichlet data on Γ .

We arrive at Bernoulli's exterior free boundary problem if the boundary Γ is the unknown. In other words, we seek a domain D with fixed boundary Σ and unknown boundary Γ such that the overdetermined boundary value problem (1.1) is solvable. This problem has many applications in engineering sciences such as fluid mechanics, see [13], or electromagnetics, see [9, 10] and references therein. In the present form, it models, for example, the growth of anodes in electrochemical processes. There exists a large amount of literature on this problem: for the existence and uniqueness of solutions, we refer the reader to e.g. [3, 4, 25], see also [12] for the related interior free boundary problem. Results concerning the geometric form of the solutions can be found in [1] and the references therein.

In the present article, we consider the free boundary problem (1.1) for the situation that the interior boundary is random, i.e., if $\Sigma = \Sigma(\omega)$ with an additional parameter $\omega \in \Omega$. Such an assumption arises when treating tolerances in fabrication processes or when the interior boundary is only known by measurements which typically contain

errors. We are thus looking for a tuple $(D(\omega), u(\omega))$ such that there holds

$$(1.2) \quad \left\{ \begin{array}{ll} \Delta u(\omega) = 0 & \text{in } D(\omega), \\ \|\nabla u(\omega)\| = f & \text{on } \Gamma(\omega), \\ u(\omega) = 0 & \text{on } \Gamma(\omega), \\ u(\omega) = 1 & \text{on } \Sigma(\omega). \end{array} \right.$$

The questions to be answered in the following are:

- (1) What is a suitable model for the domain $D(\omega)$? Is the problem well-posed in the sense of $D(\omega)$ being almost surely well-defined?
- (2) How to define the expectation of a random domain? The main difficulty to deal with here is that the space of domains is not linear.
- (3) How to compute the solution to the random free boundary problem numerically?

For sake of simplicity in representation, we restrict our consideration to the two-dimensional situation. Nonetheless, the extension to higher dimensions is straightforward.

The rest of this article is organized as follows. Section 2 is dedicated to answering the first question. We start by defining appropriate function spaces to define the stochastic model. Then, we define the random interior boundary and the resulting random outer boundary. Especially, we provide a theorem which guarantees the well-posedness of the random free boundary problem under consideration. Afterwards, we discuss the second question, i.e., the definition of the expected shape. There is no canonical definition in the literature, see [24]. Nevertheless, we require that the expectation is computable. We shall thus adopt two different points of view. The first one is a general notion of expectation for random compact sets, namely the *Vorob'ev expectation*. The second one, which is specific for the problem under consideration, is based on a parametrization of the boundary. In this case, we actually introduce the expectation and the deviation of the domain's boundaries. By analytical examples in Section 3, we show that both definitions do in general not coincide.

In Section 4, we answer the last questions. We propose in this article the use of boundary integral equations for the solution of the underlying boundary value problem. This significantly decreases the effort for the numerical solution. In particular, we can describe the related potential of the free boundary problem in terms of Green's representation formula. This also allows us to define its expectation and its deviation. For the numerical approximation of the free boundary, we propose the use of a trial method in combination with a Nyström discretization of the boundary integral equations.

Section 5 is dedicated to the numerical realization of the stochastic sampling method and the computation of the domain's statistics. This requires especially in case of the Vorob'ev expectation nontrivial numerical routines to efficiently compute level sets. In Section 6, we present numerical examples for the two different notions of expected domains in order to compare them to each other. Although the different approaches are quite different, we observe that the computed expectations are very similar for the examples under consideration. Finally, in Section 7, we state concluding remarks.

2. MODELLING UNCERTAIN DOMAINS

2.1. Notation. In the sequel, let $(\Omega, \mathcal{F}, \mathbb{P})$ denote a complete and separable probability space with σ -algebra \mathcal{F} and probability measure \mathbb{P} . Here, complete means that \mathcal{F} contains all \mathbb{P} -null sets. Then, for a given Banach space X , the *Lebesgue-Bochner space* $L_{\mathbb{P}}^p(\Omega; X)$, $1 \leq p \leq \infty$, consists of all equivalence classes of strongly measurable functions $v: \Omega \rightarrow X$ whose norm

$$\|v\|_{L_{\mathbb{P}}^p(\Omega; X)} := \begin{cases} \left(\int_{\Omega} \|v(\cdot, \omega)\|_X^p d\mathbb{P}(\omega) \right)^{1/p}, & p < \infty \\ \operatorname{ess\,sup}_{\omega \in \Omega} \|v(\cdot, \omega)\|_X, & p = \infty \end{cases}$$

is finite. If $p = 2$ and X is a separable Hilbert space, then the Bochner space is isomorphic to the tensor product space $L_{\mathbb{P}}^2(\Omega) \otimes X$. Note that, for notational convenience, we will always write $v(\phi, \omega)$ instead of $(v(\omega))(\phi)$ if $v \in L_{\mathbb{P}}^p(\Omega; X)$. For more details on Bochner spaces, we refer the reader to [20].

2.2. Vorob'ev expectation of compact sets. Let us now introduce a classical notion of expectation for a compact set. The leading idea here is to encode a random set $D(\omega)$ with its characteristic function $\mathbb{1}_{D(\omega)}$, defined by

$$\mathbb{1}_{D(\omega)}(\mathbf{x}) = \begin{cases} 1, & \text{if } \mathbf{x} \in D(\omega), \\ 0, & \text{otherwise,} \end{cases}$$

which embeds the problem into the linear space $L^\infty(\mathbb{R}^2)$. Of course, an average of characteristic functions is not a characteristic function anymore but belongs to the cone $\{q \in L^\infty(\mathbb{R}^2) : 0 \leq q \leq 1\}$. The limit object is the so-called coverage function p of the random domains $D(\omega)$ defined on \mathbb{R}^2 as

$$p(\mathbf{x}) = \mathbb{P}(\mathbf{x} \in D(\omega)).$$

An elementary remark is that the average volume of $D(\omega)$ is given by

$$\mathbb{E}[\mathcal{L}(D)] = \int_{\mathbb{R}^2} p(\mathbf{x}) \, d\mathbf{x},$$

where \mathcal{L} denotes the Lebesgue measure. The *Vorob'ev expectation* $\mathbb{E}_V[D]$ of $D(\omega)$ is then defined as a quantile of $D(\omega)$ such that its volume is $\mathbb{E}[\mathcal{L}(D)]$. More precisely, we quote the definition of [24, Definition 2.1].

Definition 2.1 (Vorob'ev expectation). *The Vorob'ev expectation $\mathbb{E}_V[D]$ of $D(\omega)$ is defined as the set $\{\mathbf{x} \in \mathbb{R}^2 : p(\mathbf{x}) \geq \mu\}$ for $\mu \in [0, 1]$ which is determined from the condition*

$$\mathcal{L}(\{\mathbf{x} \in \mathbb{R}^2 : p(\mathbf{x}) \geq \lambda\}) \leq \mathbb{E}[\mathcal{L}(D)] \leq \mathcal{L}(\{\mathbf{x} \in \mathbb{R}^2 : p(\mathbf{x}) \geq \mu\})$$

for all $\lambda > \mu$.

If there exists a $\mu \in [0, 1]$ such that the equation

$$\mathbb{E}[\mathcal{L}(D)] = \mathcal{L}(\{\mathbf{x} \in \mathbb{R}^2 : p(\mathbf{x}) \geq \mu\})$$

holds, we may simply define the Vorob'ev expectation according to

$$\mathbb{E}_V[D] = \{\mathbf{x} \in \mathbb{R}^2 : p(\mathbf{x}) \geq \mu\}.$$

Notice that, to the best of our knowledge, there exists no corresponding notion for the deviation. Nevertheless, there is the notion of the Vorob'ev deviation in order to determine how close the distribution of the random domains is to the Vorob'ev expectation, see [8].

Definition 2.2 (Vorob'ev deviation). *The Vorob'ev deviation $\mathcal{D}_V[D]$ of $D(\omega)$ is defined as the expectation of the volume of the symmetric difference between $D(\omega)$ and its Vorob'ev expectation:*

$$\mathcal{D}_V[D] = \mathbb{E} \left[\int_{\mathbb{R}^2} |\mathbf{1}_{D(\omega)}(\mathbf{x}) - \mathbf{1}_{\mathbb{E}_V[D]}(\mathbf{x})| \, d\mathbf{x} \right].$$

The next lemma shows that the Vorob'ev deviation may easily be derived from the Vorob'ev expectation and the coverage function p . It is hence easy to compute.

Lemma 2.3. *There holds*

$$\mathcal{D}_V[D] = 2 \left(\mathbb{E}[\mathcal{L}(D)] - \int_{\mathbb{E}_V[D]} p(\mathbf{x}) \, d\mathbf{x} \right) = 2 \left(\int_{\mathbb{R}^2 \setminus \mathbb{E}_V[D]} p(\mathbf{x}) \, d\mathbf{x} \right).$$

Proof. The claim is a consequence of Fubini's theorem. We have

$$\begin{aligned}
\mathcal{D}_V(D) &= \mathbb{E} \left[\int_{\mathbb{R}^2} |\mathbf{1}_{D(\omega)}(\mathbf{x}) - \mathbf{1}_{\mathbb{E}_V[D]}(\mathbf{x})|^2 d\mathbf{x} \right] \\
&= \mathbb{E} \left[\int_{\mathbb{R}^2} \mathbf{1}_{D(\omega)}(\mathbf{x}) d\mathbf{x} \right] - 2\mathbb{E} \left[\int_{\mathbb{E}_V[D]} \mathbf{1}_{D(\omega)}(\mathbf{x}) d\mathbf{x} \right] + \mathbb{E} \left[\int_{\mathbb{R}^2} \mathbf{1}_{\mathbb{E}_V[D]}(\mathbf{x}) d\mathbf{x} \right] \\
&= \mathbb{E}[\mathcal{L}(D)] - 2 \int_{\mathbb{E}_V[D]} \mathbb{E}[\mathbf{1}_{D(\omega)}(\mathbf{x})] d\mathbf{x} + \mathbb{E}[\mathcal{L}(D)] \\
&= 2 \left(\mathbb{E}[\mathcal{L}(D)] - \int_{\mathbb{E}_V[D]} p(\mathbf{x}) d\mathbf{x} \right).
\end{aligned}$$

□

2.3. Parametrization based expectation and deviation of the domain. In many applications, the interior boundary Σ is star-shaped with respect to some point. Without loss of generality, let this point be the origin $\mathbf{0}$. Then, it has a natural parametrization in polar coordinates and so does the free boundary Γ . As a consequence, the geometrical setting is embedded in some algebra of function defined on the unit circle (or the sphere in three dimensions). This allows us to define another notion of the expectation and the associated deviation. Let us make these ideas precise.

We shall assume that $\Sigma(\omega)$ is \mathbb{P} -almost surely starlike. This enables us to parameterize this random boundary in accordance with

$$(2.3) \quad \Sigma(\omega) = \{ \mathbf{x} = \boldsymbol{\sigma}(\phi, \omega) \in \mathbb{R}^2 : \boldsymbol{\sigma}(\phi, \omega) = q(\phi, \omega) \mathbf{e}_r(\phi), \phi \in I \}.$$

Here, $\mathbf{e}_r(\phi) := [\cos(\phi), \sin(\phi)]^\top$ is the radial direction and $I := [0, 2\pi]$ is the parameter interval. The radial function $q(\phi, \omega) \geq \underline{c} > 0$ has to be in the Lebesgue-Bochner space $L^2(\Omega; C_{\text{per}}^2(I))$, where $C_{\text{per}}^2(I)$ denotes the Banach space of periodic, twice continuously differentiable functions, i.e.,

$$C_{\text{per}}^2(I) := \{ f \in C(I) : f^{(i)}(0) = f^{(i)}(2\pi), i = 0, 1, 2 \},$$

equipped with the norm

$$\|f\|_{C_{\text{per}}^2(I)} := \sum_{i=0}^2 \max_{x \in I} |f^{(i)}(x)|.$$

If the interior boundary $\Sigma(\omega)$ is starlike, then also the exterior boundary $\Gamma(\omega)$ is starlike. In particular, it follows that the free boundary $\Gamma(\omega)$ is C^∞ -smooth, see [2] for details. Hence, the exterior boundary can likewise be represented via its parameterization:

$$(2.4) \quad \Gamma(\omega) = \{ \mathbf{x} = \boldsymbol{\gamma}(\phi, \omega) \in \mathbb{R}^2 : \boldsymbol{\gamma}(\phi, \omega) = r(\phi, \omega) \mathbf{e}_r(\phi), \phi \in I \}.$$

The following theorem guarantees us the well-posedness of the problem under consideration, cf. [4, 25]. It shows that there holds $r(\phi, \omega) \in L_{\mathbb{P}}^{\infty}(\Omega, C_{\text{per}}^2(I))$ if $q(\phi, \omega)$ is almost surely bounded. In this case, the function $\gamma(\phi, \omega)$ is well defined.

Theorem 2.4. *Assume that $q(\phi, \omega)$ is uniformly bounded almost surely, i.e.,*

$$(2.5) \quad q(\phi, \omega) \leq \underline{R} \quad \text{for all } \phi \in I \text{ and } \mathbb{P}\text{-almost every } \omega \in \Omega.$$

Then, there exists a unique solution $(D(\omega), u(\omega))$ to (1.2) for almost every $\omega \in \Omega$. Especially, with some constant $\bar{R} > \underline{R}$, the radial function $r(\phi, \omega)$ of the associated free boundary (2.4) satisfies

$$q(\phi, \omega) < r(\phi, \omega) \leq \bar{R} \quad \text{for all } \phi \in I \text{ and } \mathbb{P}\text{-almost every } \omega \in \Omega.$$

Proof. In view of (2.5), it follows that

$$\Sigma(\omega) \subset B_{\underline{R}}(\mathbf{0}) := \{\mathbf{x} \in \mathbb{R}^2 : \|\mathbf{x}\| < \underline{R}\}$$

for almost every $\omega \in \Omega$. Hence, for fixed $\omega \in \Omega$, [25, Theorem 1] guarantees the unique solvability of (1.2). In particular, there exists a constant $\bar{R} > \underline{R}$ such that $\Gamma(\omega) \subset B_{\bar{R}}(\mathbf{0})$ whenever $\Sigma(\omega) \subset B_{\underline{R}}(\mathbf{0})$. Therefore, the claim follows since $q(\phi, \omega)$ is supposed to be uniformly bounded in $\omega \in \Omega$. \square

Having the parameterizations $\sigma(\omega)$ and $\gamma(\omega)$ at hand, we can define the expectation and the variance of the boundary then of domain $D(\omega)$. Notice that the definition of the expectation is also called the radius-vector expectation, see [24, Section 2.4].

Definition 2.5 (Parametrization based expectation of the boundary). *The parametrization based expectation $\mathbb{E}_{\mathcal{P}}[D]$ of the boundaries $\Sigma(\omega)$ and $\Gamma(\omega)$ is given by*

$$\begin{aligned} \mathbb{E}_{\mathcal{P}}[\Sigma] &= \{\mathbf{x} \in \mathbb{R}^2 : \mathbf{x} = \mathbb{E}[q](\phi)\mathbf{e}_r(\phi), \phi \in I\}, \\ \mathbb{E}_{\mathcal{P}}[\Gamma] &= \{\mathbf{x} \in \mathbb{R}^2 : \mathbf{x} = \mathbb{E}[r](\phi)\mathbf{e}_r(\phi), \phi \in I\}. \end{aligned}$$

Having the expectation of the boundary at hand, we can define the expected domain just as the annular domain determined by the expected interior boundary and the expected outer boundary.

Definition 2.6 (Parametrization based expectation of the domain). *In accordance with the parametrization based expectations of its boundaries $\Sigma(\omega)$ and $\Gamma(\omega)$, the parametrization based expectation $\mathbb{E}_{\mathcal{P}}[D]$ of the domain $D(\omega)$ is given by*

$$\mathbb{E}_{\mathcal{P}}[D] = \{\mathbf{x} = (\rho, \phi) \in \mathbb{R}^2 : \mathbb{E}[q](\phi) \leq \rho \leq \mathbb{E}[r](\phi)\}.$$

The Vorob'ev expectation and the parametrization based expectation of the domain lead in general to different results. As an example, we consider the random disk $D(\omega)$ of fixed center $\mathbf{0}$ with random radius $r(\omega)$. Thus, it is obvious that the expected domains are disks as well. More precisely, we have

$$\mathbb{E}_{\mathcal{V}}[D] = B(\mathbf{0}, \sqrt{\mathbb{E}[r^2]}) \quad \text{and} \quad \mathbb{E}_{\mathcal{P}}[D] = B(\mathbf{0}, \mathbb{E}[r]),$$

respectively. In the model case where r is uniformly distributed on $[R_1, R_2]$, we obtain

$$\sqrt{\mathbb{E}[r^2]} = \sqrt{\frac{1}{3} \frac{R_2^3 - R_1^3}{R_2 - R_1}} = \sqrt{\frac{R_1^2 + R_1 R_2 + R_2^2}{3}},$$

whereas

$$\mathbb{E}[r] = \frac{R_1 + R_2}{2}.$$

We shall next define the notion of the parametrization based deviation for $\Sigma(\omega)$ and $\Gamma(\omega)$.

Definition 2.7 (Parametrization based deviation of the boundary). *The parametrization based deviation $\mathcal{D}_{\mathcal{P}}[D]$ of the boundaries $\Sigma(\omega)$ and $\Gamma(\omega)$ is given by*

$$\begin{aligned} \mathcal{D}_{\mathcal{P}}[\Sigma] &= \sqrt{\mathbb{E}[\|q - \mathbb{E}[q]\|_{L^\infty(I)}^2]}, \\ \mathcal{D}_{\mathcal{P}}[\Gamma] &= \sqrt{\mathbb{E}[\|r - \mathbb{E}[r]\|_{L^\infty(I)}^2]}. \end{aligned}$$

The main interest of this definition is to obtain a Bienaymé-Chebyshev inequality for boundaries. Indeed, we have the following statement:

Lemma 2.8. *Let $\Psi \in \{\Sigma(\omega), \Gamma(\omega)\}$ with parametrization $\psi(\phi, \omega) = p(\phi, \omega)\mathbf{e}_r(\phi)$ and denote by $\mathcal{T}_\rho(\mathbb{E}_{\mathcal{P}}[\Psi])$ the following tubular neighborhood of the parametrization based expectation of the boundary:*

$$\mathcal{T}_\rho(\mathbb{E}_{\mathcal{P}}[\Psi]) = \{\mathbf{x}(\phi) = \tau\mathbf{e}_r(\phi) \in \mathbb{R}^2 : |\mathbb{E}[p](\phi) - \tau| \leq \rho, \phi \in I\}.$$

Then, for any $k > 0$, one has

$$\mathbb{P}[\Psi \notin \mathcal{T}_{k\mathcal{D}_{\mathcal{P}}[\Psi]}(\mathbb{E}_{\mathcal{P}}[\Psi])] \leq \frac{1}{k^2},$$

Proof. Without loss of generality, we consider the case $\Psi = \Sigma$. The condition $\Psi \notin \mathcal{T}_{k\mathcal{D}_{\mathcal{P}}[\Psi]}(\mathbb{E}_{\mathcal{P}}[\Psi])$ is satisfied if there is a $\phi \in I$ such that $|q(\phi, \omega) - \mathbb{E}[q](\phi)| \geq k\mathcal{D}_{\mathcal{P}}[\Psi]$. Therefore, it holds $\|q(\cdot, \omega) - \mathbb{E}[q]\|_\infty \geq k\mathcal{D}_{\mathcal{P}}[\Psi]$. The conclusion follows now from the usual Bienaymé-Chebyshev inequality. \square

When we consider the domain itself, things become more complicated since one has to take into account the deviations of both boundaries. They are strongly correlated since the outer boundary is uniquely defined by the interior boundary. However, the dependance is very complex and we use the crude estimate

$$\begin{aligned} & \mathbb{P}[\Sigma \not\subset \mathcal{T}_{k_\Sigma \mathcal{D}_P[\Sigma]}(\mathbb{E}_P[\Sigma]) \text{ or } \Gamma \not\subset \mathcal{T}_{k_\Gamma \mathcal{D}_P[\Gamma]}(\mathbb{E}_P[\Gamma])] \\ & \leq \mathbb{P}[\Sigma \not\subset \mathcal{T}_{k_\Sigma \mathcal{D}_P[\Sigma]}(\mathbb{E}_P[\Sigma])] + \mathbb{P}[\Gamma \not\subset \mathcal{T}_{k_\Gamma \mathcal{D}_P[\Gamma]}(\mathbb{E}_P[\Gamma])] = \frac{1}{k_\Sigma^2} + \frac{1}{k_\Gamma^2}. \end{aligned}$$

As a consequence, we can derive a version of Lemma 2.8 for the annular domain. To that end, we introduce some notation. Let $\rho_\Sigma, \rho_\Gamma > 0$ and set

$$\begin{aligned} \mathbb{E}_P[D]_{\rho_\Sigma, \rho_\Gamma}^+ &= \mathbb{E}_P[D] \cup (S_1 \cup S_2), \\ \mathbb{E}_P[D]_{\rho_\Sigma, \rho_\Gamma}^- &= \mathbb{E}_P[D] \setminus (S_1 \cup S_2), \end{aligned}$$

where

$$S_1 := \{\mathbf{x} \in \mathbb{R}^2 : \text{dist}(\mathbf{x}, \mathbb{E}_P[\Sigma]) < \rho_\Sigma\} \quad \text{and} \quad S_2 := \{\mathbf{x} \in \mathbb{R}^2 : \text{dist}(\mathbf{x}, \mathbb{E}_P[\Gamma]) < \rho_\Gamma\},$$

so that the event $\Sigma \not\subset \mathcal{T}_{k_\Sigma \mathcal{D}_P[\Sigma]}(\mathbb{E}_P[\Sigma])$ or $\Gamma \not\subset \mathcal{T}_{k_\Gamma \mathcal{D}_P[\Gamma]}(\mathbb{E}_P[\Gamma])$ induces also the event $D \not\subset \mathbb{E}_P[D]_{k_\Sigma \mathcal{D}_P(\Sigma), k_\Gamma \mathcal{D}_P(\Gamma)}^+$ or $\mathbb{E}_P[D]_{k_\Sigma \mathcal{D}_P(\Sigma), k_\Gamma \mathcal{D}_P(\Gamma)}^- \not\subset D$. This immediately implies the following

Lemma 2.9. *For any $k_\Sigma, k_\Gamma > 0$, one has*

$$\mathbb{P}[D \not\subset \mathbb{E}_P[D]_{k_\Sigma \mathcal{D}_P(\Sigma), k_\Gamma \mathcal{D}_P(\Gamma)}^+ \text{ or } \mathbb{E}_P[D]_{k_\Sigma \mathcal{D}_P(\Sigma), k_\Gamma \mathcal{D}_P(\Gamma)}^- \not\subset D] \leq \frac{1}{k_\Sigma^2} + \frac{1}{k_\Gamma^2}.$$

The inconvenience of Lemma 2.8 is that the width of the tubular neighbourhood is uniform along the expected boundary. If one is, however, interested in what happens along a specific direction, one can use the pointwise variation introduced in [16].

3. ANALYTICAL COMPUTATIONS IN THE CASE OF CONCENTRIC ANNULI

The calculations can be performed analytically if the interior boundary Σ is a circle around the origin with radius q . Then, due to symmetry, also the free boundary Γ will be a circle around the origin with unknown radius r .

3.1. Solution of the deterministic free boundary problem. Using polar coordinates and making the ansatz $u(\rho, \phi) = y(\rho)$, the solution with respect to the prescribed Dirichlet boundary condition of (1.1) is given in the case of dimension two by

$$y(\rho) = \frac{\log\left(\frac{\rho}{r}\right)}{\log\left(\frac{q}{r}\right)}.$$

The desired Neumann boundary condition at the free boundary r yields the equation

$$-y'(r) = \frac{1}{r \log\left(\frac{r}{q}\right)} = f,$$

which can be solved by means of Lambert's W -function:

$$r = F(q) := \frac{1}{fW\left(\frac{1}{fq}\right)}.$$

Let us recall that Lambert's W -function is the inverse of $x \mapsto xe^x$. It is a non-decreasing function on $(0, +\infty)$ which, however, provides a non-analytic expression. An important remark is that the solution map $F : q \mapsto r(q)$ is invertible with inverse

$$(3.6) \quad F^{-1} : t \mapsto te^{-\frac{1}{ft}}.$$

Notice that a similar computation can be performed in the case of dimension three. The potential is then

$$y(\rho) = \frac{qr}{r-q} \left(\frac{1}{\rho} - \frac{1}{r} \right).$$

Thus, free boundary condition yields

$$r = \frac{qf + \sqrt{(fq)^2 + 4fq}}{2f}.$$

3.2. Random interior radius with discontinuous density. Let us now consider the case where q switches between q_{\min} and q_{\max} with the probability $\mathbb{P}(q = q_{\min}) = \mathbb{P}(q = q_{\max}) = 1/2$. Then, of course, also the outer boundary switches between $F(q_{\min})$ and $F(q_{\max})$ with equal probability. If $q_{\max} \leq F(q_{\min})$, then the coverage is simply given by

$$p(\mathbf{x}) = \begin{cases} \frac{1}{2}, & \text{if } q_{\min} \leq \|\mathbf{x}\| \leq q_{\max} \text{ or } F(q_{\min}) \leq \|\mathbf{x}\| \leq F(q_{\max}), \\ 1, & \text{if } q_{\max} \leq \|\mathbf{x}\| \leq F(q_{\min}), \\ 0, & \text{elsewhere.} \end{cases}$$

As one readily verifies by Definition 2.1, the Vorob'ev expectation is the annulus which is bounded by the circles with radii q_{\min} and $F(q_{\max})$. Whereas, the parametrization based expectation is the annulus which is bounded by the circles with radii $(q_{\min} + q_{\max})/2$ and $(F(q_{\min}) + F(q_{\max}))/2$. We refer the reader to Figure 3.2 for a visualization of the current situation.

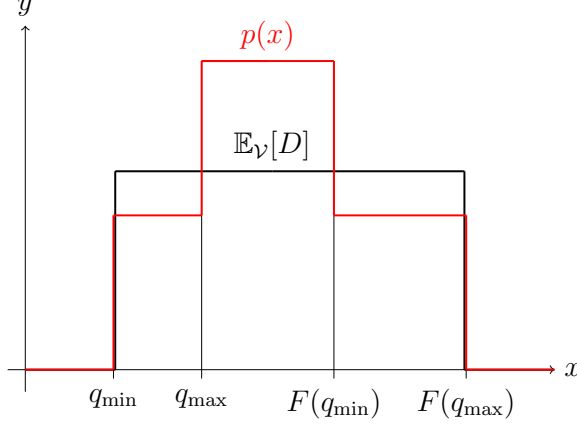


FIGURE 3.2. Coverage function and the Vorob'ev expectation in case of a discrete density and an annulus.

3.3. Random interior radius with continuous density. Let us now consider the case where q is random with a given distribution with values in the compact set $[q_{\min}, q_{\max}]$ where $0 < q_{\min} < q_{\max}$. Assume that the interior radius q has the probability density \mathbf{q} . The random domain is obviously the annulus

$$D(\omega) = \{\mathbf{x} \in \mathbb{R}^2 : q(\omega) \leq \|\mathbf{x}\| \leq F(q(\omega))\}.$$

The outer boundary radii vary in $[F(q_{\min}), F(q_{\max})]$ by the monotony of F . By definition, the parametrization based expectation is then simply the annulus

$$\mathbb{E}_{\mathcal{P}}[D] = \{\mathbf{x} \in \mathbb{R}^2 : \mathbb{E}[q] \leq \|\mathbf{x}\| \leq \mathbb{E}[F(q)]\}.$$

Let us next compute the Vorob'ev expectation. To that end, we determine the coverage function. If $\|\mathbf{x}\| \notin [q_{\min}, F(q_{\max})]$, then $p(\mathbf{x}) = 0$. For $\|\mathbf{x}\| \in [q_{\min}, F(q_{\max})]$, one has

$$\begin{aligned} p(\mathbf{x}) &= \mathbb{P}[\mathbf{x} \in D] \\ &= \mathbb{P}[q \leq \|\mathbf{x}\| \leq F(q)] \\ &= \mathbb{P}[\{q \leq \|\mathbf{x}\|\} \cap \{\|\mathbf{x}\| \leq F(q)\}]. \end{aligned}$$

Then, noticing that $\{\|\mathbf{x}\| \leq F(q)\} = \{F^{-1}(\|\mathbf{x}\|) \leq q\}$, we get

$$\begin{aligned} p(\mathbf{x}) &= \mathbb{P}[\{q \leq \|\mathbf{x}\|\} \cap \{F^{-1}(\|\mathbf{x}\|) \leq q\}] \\ &= \mathbb{P}[F^{-1}(\|\mathbf{x}\|) \leq q \leq \|\mathbf{x}\|] \\ &= \int_{F^{-1}(\|\mathbf{x}\|)}^{\|\mathbf{x}\|} \mathbf{q}(t) dt. \end{aligned}$$

Herein, \mathbf{q} denotes the probability density of q . Thanks to the expression (3.6) of the reciprocal function, we get

$$p(\mathbf{x}) = \int_{\|\mathbf{x}\|e^{-1/f\|\mathbf{x}\|}}^{\|\mathbf{x}\|} \mathbf{q}(t) dt.$$

Obviously, the coverage function p is radially symmetric. The Vorob'ev expected domain $\mathbb{E}_{\mathcal{V}}[D]$ is thus an annulus of the expected volume

$$\mathbb{E}[\mathcal{L}(D)] = \pi \left(\frac{1}{f^2} \mathbb{E} \left[\frac{1}{W(\frac{1}{fq})^2} \right] - \mathbb{E}[q^2] \right).$$

Nevertheless, the inner and outer radii of $\mathbb{E}_{\mathcal{V}}[D]$ depend on the density \mathbf{q} and their general computation is not trivial. We shall illustrate this by the uniform distribution $\mathbf{q} \equiv 1/(q_{\max} - q_{\min})$ on $[q_{\min}, q_{\max}]$. Since

$$p(\mathbf{x}) = \frac{1}{q_{\max} - q_{\min}} \int_{\|\mathbf{x}\|e^{-1/f\|\mathbf{x}\|}}^{\|\mathbf{x}\|} \mathbf{1}_{[q_{\min}, q_{\max}]} dt.$$

The coverage function is piecewise linear with critical points q_{\min} , q_{\max} , $F(q_{\min})$ and $F(q_{\max})$.

We assume that $q_{\max} \leq F(q_{\min})$. Then, we have

$$p(\mathbf{x}) = \begin{cases} \frac{\|\mathbf{x}\| - q_{\min}}{q_{\max} - q_{\min}}, & \text{if } q_{\min} \leq \|\mathbf{x}\| \leq q_{\max}, \\ 1, & \text{if } q_{\max} \leq \|\mathbf{x}\| \leq F(q_{\min}), \\ \frac{q_{\max} - \|\mathbf{x}\|e^{-1/f\|\mathbf{x}\|}}{q_{\max} - q_{\min}}, & \text{if } F(q_{\min}) \leq \|\mathbf{x}\| \leq F(q_{\max}), \\ 0, & \text{elsewhere.} \end{cases}$$

This density is visualized in Figure 3.3.

We shall next calculate the Lebesgue measure of the level set $\{p \geq \mu\}$ for given $0 < \mu < 1$. To that end, notice that $p(\mathbf{x}) \geq \mu$ implies

$$\frac{\|\mathbf{x}\| - q_{\min}}{q_{\max} - q_{\min}} \geq \mu \quad \text{and} \quad \frac{q_{\max} - \|\mathbf{x}\|e^{-1/f\|\mathbf{x}\|}}{q_{\max} - q_{\min}} \geq \mu.$$

Therefore, we conclude

$$\mu q_{\max} + (1 - \mu)q_{\min} \leq \|\mathbf{x}\| \leq F((1 - \mu)q_{\max} + \mu q_{\min}),$$

which gives

$$\mathcal{L}(\{\mathbf{x} \in \mathbb{R}^2 : p(\mathbf{x}) \geq \lambda\}) = \pi \left[F((1 - \mu)q_{\max} + \mu q_{\min})^2 - (\mu q_{\max} + (1 - \mu)q_{\min})^2 \right].$$

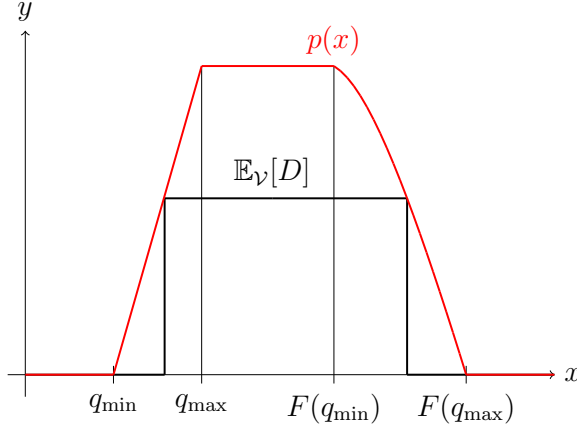


FIGURE 3.3. Coverage function and the Vorob'ev expectation in case of a uniform density and an annulus.

The Vorob'ev expectation $\mathbb{E}_V[D]$ of D is finally the level set $\{p \geq \mu^*\}$, where μ^* is determined from the condition

$$\mathbb{E}[F(q)^2] - \mathbb{E}[q^2] = F((1 - \mu^*)q_{\max} + \mu^*q_{\min})^2 - (\mu^*q_{\max} + (1 - \mu^*)q_{\min})^2.$$

Herein, we have

$$\mathbb{E}[q^2] = \frac{q_{\max}^2 + q_{\max}q_{\min} + q_{\min}^2}{3} \quad \text{and} \quad \mathbb{E}[F(q)^2] = \mathbb{E}\left[\frac{1}{f^2W(\frac{1}{fq})^2}\right].$$

4. COMPUTING FREE BOUNDARIES

4.1. Trial method. In order to compute the expectation and the deviation of the domain $D(\omega)$, we have to be able to determine the free boundary $\Gamma(\omega)$ for each specific realization $\omega \in \Omega$ of the interior boundary $\Sigma(\omega)$. To that end, we employ the so-called trial method, which is a fixed point type iterative method. For sake of simplicity in representation, we omit the random parameter $\omega \in \Omega$ in this section, i.e., we assume that $\omega \in \Omega$ is fixed.

The trial method for the solution of the free boundary problem (1.1) requires an update rule. Suppose that the current boundary in the k -th iteration is Γ_k and let the current state u_k satisfy

$$(4.7) \quad \begin{aligned} \Delta u_k &= 0 && \text{in } D_k, \\ u_k &= 1 && \text{on } \Sigma, \\ -\frac{\partial u_k}{\partial \mathbf{n}} &= f && \text{on } \Gamma_k. \end{aligned}$$

In this case, the updated boundary Γ_{k+1} is determined by modifying the old boundary Γ_k with respect to the radial direction. This is achieved by the update rule

$$\gamma_{k+1} = \gamma_k + \delta r_k \mathbf{e}_r.$$

The increment function $\delta r_k \in C_{\text{per}}^2([0, 2\pi])$ is chosen such that the desired homogeneous Dirichlet boundary condition is approximately satisfied at the updated boundary Γ_{k+1} , i.e.,

$$(4.8) \quad 0 \stackrel{!}{=} u_k \circ \gamma_{k+1} \approx u_k \circ \gamma_k + \left(\frac{\partial u_k}{\partial \mathbf{e}_r} \circ \gamma_k \right) \delta r_k \quad \text{on } [0, 2\pi],$$

where u_k is supposed to be smoothly extended into the exterior of the domain D_k . For numerical reasons, we decompose the derivative of u_k in the direction \mathbf{e}_r into its normal and tangential components

$$(4.9) \quad \frac{\partial u_k}{\partial \mathbf{e}_r} = \frac{\partial u_k}{\partial \mathbf{n}} \langle \mathbf{e}_r, \mathbf{n} \rangle + \frac{\partial u_k}{\partial \mathbf{t}} \langle \mathbf{e}_r, \mathbf{t} \rangle \quad \text{on } \Gamma_k$$

to arrive finally at the following iterative scheme (cf. [12, 27, 15]):

- (1) Choose an initial guess Γ_0 of the free boundary.
- (2a) Solve the boundary value problem with the Neumann boundary condition on the free boundary Γ_k .
- (2b) Update the free boundary Γ_k such that the Dirichlet boundary condition is approximately satisfied at the new boundary Γ_{k+1} :

$$(4.10) \quad \delta r_k = - \frac{u_k}{\frac{\partial u_k}{\partial \mathbf{e}_r}} = - \frac{u_k}{f \langle \mathbf{n}, \mathbf{e}_r \rangle + \frac{\partial u_k}{\partial \mathbf{t}} \langle \mathbf{t}, \mathbf{e}_r \rangle}$$

- (3) Repeat step (2) until the process becomes stationary up to a specified accuracy.

Notice that the update equation (4.10) is always solvable at least in a neighbourhood of the optimum free boundary Γ since there it holds $-\partial u / \partial \mathbf{e}_r = f \langle \mathbf{e}_r, \mathbf{n} \rangle > 0$ due to $\partial u_k / \partial \mathbf{t} = 0$, $f > 0$ and $\langle \mathbf{e}_r, \mathbf{n} \rangle > 0$ for starlike domains.

4.2. Discretizing the free boundary. For the numerical computations, we discretize the radial function r_k associated with the boundary Γ_k by a trigonometric polynomial according to

$$(4.11) \quad r_k(\phi) = \frac{a_0}{2} + \sum_{\ell=1}^{p-1} \{a_\ell \cos(\ell\phi) + b_\ell \sin(\ell\phi)\} + \frac{a_p}{2} \cos(p\phi).$$

This obviously ensures that r_k is always an element of $C_{\text{per}}^2(I)$. To determine the increment function δr_k , represented likewise by a trigonometric polynomial, we insert

the $m \geq 2n$ equidistantly distributed points $\phi_i = 2\pi i/m$ into the update equation (4.10):

$$\delta r_k = -\frac{u_k}{f\langle \mathbf{n}, \mathbf{e}_r \rangle + \frac{\partial u_k}{\partial \mathbf{t}} \langle \mathbf{t}, \mathbf{e}_r \rangle} \quad \text{in all the points } \phi_1, \dots, \phi_m.$$

This is a discrete least-squares problem which can simply be solved by the normal equations. In view of the orthogonality of the Fourier basis, this means just a truncation of the respective trigonometric polynomial.

4.3. Boundary integral equations. Our approach to determine the solution u_k of the state equation (4.7) relies on the reformulation as a boundary integral equation by employing the Green's function for the Laplacian

$$G(\mathbf{x}, \mathbf{y}) = -\frac{1}{2\pi} \log \|\mathbf{x} - \mathbf{y}\|_2.$$

Namely, the solution $u_k(\mathbf{x})$ of (4.7) is given in each point $\mathbf{x} \in D$ by Green's representation formula

$$(4.12) \quad u_k(\mathbf{x}) = \int_{\Gamma_k \cup \Sigma} \left\{ G(\mathbf{x}, \mathbf{y}) \frac{\partial u_k}{\partial \mathbf{n}}(\mathbf{y}) - \frac{\partial G(\mathbf{x}, \mathbf{y})}{\partial \mathbf{n}_\mathbf{y}} u_k(\mathbf{y}) \right\} d\sigma_\mathbf{y}.$$

Using the jump properties of the layer potentials, we obtain the direct boundary integral formulation of the problem

$$(4.13) \quad \frac{1}{2} u_k(\mathbf{x}) = \int_{\Gamma_k \cup \Sigma} G(\mathbf{x}, \mathbf{y}) \frac{\partial u_k}{\partial \mathbf{n}}(\mathbf{y}) d\sigma_\mathbf{y} - \int_{\Gamma_k \cup \Sigma} \frac{\partial G(\mathbf{x}, \mathbf{y})}{\partial \mathbf{n}_\mathbf{y}} u_k(\mathbf{y}) d\sigma_\mathbf{y},$$

where $\mathbf{x} \in \Gamma_k \cup \Sigma$. If we label the boundaries by $A, B \in \{\Gamma_k, \Sigma\}$, then (4.13) includes the single layer operator

$$(4.14) \quad \mathcal{V} : C(A) \rightarrow C(B), \quad (\mathcal{V}_{AB}\rho)(\mathbf{x}) = -\frac{1}{2\pi} \int_A \log \|\mathbf{x} - \mathbf{y}\|_2 \rho(\mathbf{y}) d\sigma_\mathbf{y}$$

and the double layer operator

$$(4.15) \quad \mathcal{K} : C(A) \rightarrow C(B), \quad (\mathcal{K}_{AB}\rho)(\mathbf{x}) = \frac{1}{2\pi} \int_A \frac{\langle \mathbf{x} - \mathbf{y}, \mathbf{n}_\mathbf{y} \rangle}{\|\mathbf{x} - \mathbf{y}\|_2^2} \rho(\mathbf{y}) d\sigma_\mathbf{y}$$

with the densities $\rho \in C(A)$ being the Cauchy data of u on A . The equation (4.13) in combination with (4.14) and (4.15) indicates the Neumann-to-Dirichlet map, which for problem (4.7) induces the following system of integral equations:

$$(4.16) \quad \begin{bmatrix} \frac{1}{2}I + \mathcal{K}_{\Gamma\Gamma} & -\mathcal{V}_{\Sigma\Gamma} \\ \mathcal{K}_{\Gamma\Sigma} & -\mathcal{V}_{\Sigma\Sigma} \end{bmatrix} \begin{bmatrix} u_k|_\Gamma \\ \frac{\partial u_k}{\partial \mathbf{n}}|_\Sigma \end{bmatrix} = \begin{bmatrix} \mathcal{V}_{\Gamma\Gamma} & -\mathcal{K}_{\Sigma\Gamma} \\ \mathcal{V}_{\Gamma\Sigma} & -(\frac{1}{2}I + \mathcal{K}_{\Sigma\Sigma}) \end{bmatrix} \begin{bmatrix} -f \\ 1 \end{bmatrix}.$$

The boundary integral operator on the left hand side of this coupled system of boundary integral equation is continuous and satisfies a Gårding inequality with respect to the product Sobolev space $L^2(\Gamma) \times H^{-1/2}(\Sigma)$ provided that $\text{diam}(D) < 1$. Since its injectivity follows from potential theory, this system of integral equations is uniquely solvable according to the Riesz-Schauder theory.

The next step to the solution of the boundary value problem is the numerical approximation of the integral operators included in (4.16) which first requires the parameterization of the integral equations. To that end, we insert the parameterizations σ and γ_k of the boundaries Σ and Γ_k , respectively. For the approximation of the unknown Cauchy data, we use the collocation method based on trigonometric polynomials. Applying the trapezoidal rule for the numerical quadrature and the regularization technique along the lines of [22] to deal with the singular integrals, we arrive at an exponentially convergent Nyström method provided that the data and the boundaries and thus the solution are arbitrarily smooth.

5. COMPUTING THE DOMAINS STATISTICS

5.1. Random model for the interior boundary. For computational purposes, it is convenient to describe the interior boundary $\Sigma(\omega)$ by its radial function $q(\phi, \omega)$ in accordance with (2.3). We assume that we are given its expectation

$$\mathbb{E}[q](\phi) = \int_{\Omega} q(\phi, \omega) d\mathbb{P}(\omega)$$

and its covariance

$$\begin{aligned} \text{Cov}[q](\phi, \phi') &= \mathbb{E}[q(\phi, \cdot)q(\phi', \cdot)] - \mathbb{E}[q](\phi)\mathbb{E}[q](\phi') \\ &= \int_{\Omega} q(\phi, \omega)q(\phi', \omega) d\mathbb{P}(\omega) - \mathbb{E}[q](\phi)\mathbb{E}[q](\phi'). \end{aligned}$$

In accordance with [23], the radial function $q(\phi, \omega)$ can be represented by the so called *Karhunen-Loève expansion*

$$q(\phi, \omega) = \mathbb{E}[q](\phi) + \sum_{k=1}^N q_k(\phi)Y_k(\omega).$$

Herein, the functions $\{q_k(\phi)\}_k$ are scaled versions of the eigenfunctions of the Hilbert-Schmidt operator associated to $\text{Cov}[q](\phi, \phi')$. Common approaches to numerically recover the Karhunen-Loève expansion from these quantities are given in e.g. [17] and the references therein. By construction, the random variables $\{Y_k(\omega)\}_k$ in the Karhunen-Loève expansion are uncorrelated. For our modelling, we suppose them also to be independent and identically distributed with $\text{img } Y_k(\omega) = [-1, 1]$.

For numerical simulation, we aim at approximating the domains statistics with the aid of a (quasi-) Monte Carlo quadrature. To that end, we first parameterize the stochastic influences in $q(\phi, \omega)$ by considering the parameter domain $\square := [-1, 1]^N$ and setting

$$q(\phi, \mathbf{y}) = \mathbb{E}[q](\phi) + \sum_{k=1}^N q_k(\phi)y_k \quad \text{for } \mathbf{y} = [y_1, \dots, y_N]^T \in \square.$$

Especially, we have $q(\phi, \mathbf{y}) \in L^\infty(\square; C_{\text{per}}^2(I))$ if $q(\phi, \omega) \in L^\infty(\Omega; C_{\text{per}}^2(I))$. Here, the space $L^\infty(\square; C_{\text{per}}^2(I))$ is equipped with the pushforward measure $\mathbb{P}_{\mathbf{Y}}$, where $\mathbf{Y} = [Y_1, \dots, Y_N]^\top$. This measure is of product structure due to the independence of the random variables. If the measure $\mathbb{P}_{\mathbf{Y}}$ is absolutely continuous with respect to the Lebesgue measure, then there exists a density $\rho(\mathbf{y})$, which is also of product structure, such that there holds

$$\mathbb{E}_{\mathcal{P}}[\Sigma](\phi) = \mathbb{E}[q](\phi) = \int_{\Omega} q(\phi, \omega) d\mathbb{P}(\omega) = \int_{\square} q(\phi, \mathbf{y}) \rho(\mathbf{y}) d\mathbf{y}.$$

5.2. Sampling methods. Having parametrized the random problem under consideration, we can apply sampling methods to compute the high-dimensional integrals required for evaluating statistical quantities. Both, the Monte Carlo quadrature and the quasi-Monte Carlo quadrature, approximate the integral of a sufficiently smooth function f over \square by a weighted sum according to

$$\int_{\square} f(\mathbf{y}) d\mathbf{y} \approx \frac{1}{M} \sum_{i=1}^M f(\mathbf{y}_i).$$

Herein, the sample points $\{\mathbf{y}_1, \dots, \mathbf{y}_M\}$ are either chosen randomly with respect to the uniform distribution, which results in the Monte Carlo quadrature, or deterministically with respect to a low-discrepancy sequence, which results in the quasi-Monte Carlo quadrature. The Monte Carlo quadrature can be shown to converge, in the mean square sense, with a dimension independent rate of $M^{-1/2}$. The quasi-Monte Carlo quadrature based, for example, on Halton points, cf. [14], converges instead with the rate $M^{\delta-1}$ for arbitrary $\delta > 0$. Although, for the quasi-Monte Carlo quadrature, the integrand has to provide bounded first order mixed derivatives. For more details on this topic, see [7] and the references therein.

Recall that

$$F: L^\infty(\Omega; C_{\text{per}}^2(I)) \rightarrow L^\infty(\Omega; C_{\text{per}}^2(I)), \quad q(\phi, \omega) \mapsto r(\phi, \omega)$$

denotes the solution map which maps the interior radial function uniquely to the exterior radial function. Thus, for any sample $\mathbf{y}_i \in \square$, the random domain $D(\mathbf{y}_i)$ is uniquely described as the annulus bounded by $\Sigma(\mathbf{y}_i)$ and $\Gamma(\mathbf{y}_i)$, given by

$$\begin{aligned} \Sigma(\mathbf{y}_i) &= \{\mathbf{x} \in \mathbb{R}^2 : \mathbf{x} = q(\cdot, \mathbf{y}_i) \mathbf{e}_r(\phi), \phi \in I\}, \\ \Gamma(\mathbf{y}_i) &= \{\mathbf{x} \in \mathbb{R}^2 : \mathbf{x} = F(q(\cdot, \mathbf{y}_i)) \mathbf{e}_r(\phi), \phi \in I\}. \end{aligned}$$

The parametric expectations $\mathbb{E}_{\mathcal{P}}[\Sigma]$, $\mathbb{E}_{\mathcal{P}}[\Gamma]$, and $\mathbb{E}_{\mathcal{P}}[D]$ can hence be computed in accordance with Definitions 2.5 and 2.6 by making use of the approximations

$$\begin{aligned}\mathbb{E}[q](\phi) &\approx \frac{1}{M} \sum_{i=1}^M q(\phi, \mathbf{y}_i) \rho(\mathbf{y}_i), \\ \mathbb{E}[r](\phi) &\approx \frac{1}{M} \sum_{i=1}^M F(q(\phi, \mathbf{y}_i)) \rho(\mathbf{y}_i).\end{aligned}$$

The deviation $\mathcal{D}_{\mathcal{P}}[\Sigma]$ and $\mathcal{D}_{\mathcal{P}}[\Gamma]$ of the domain are computed in accordance with

$$\begin{aligned}\mathcal{D}_{\mathcal{P}}[\Sigma] &\approx \frac{1}{M} \sqrt{\sum_{i=1}^M \left(\max_{\phi \in [0, 2\pi]} |q(\phi, \mathbf{y}_i) - \mathbb{E}[q](\phi)| \right)^2}, \\ \mathcal{D}_{\mathcal{P}}[\Gamma] &\approx \frac{1}{M} \sqrt{\sum_{i=1}^M \left(\max_{\phi \in [0, 2\pi]} |F(q(\phi, \mathbf{y}_i)) - \mathbb{E}[r](\phi)| \right)^2}.\end{aligned}$$

Notice that the L^∞ -norm of a function is approximated by evaluating the function in many points $\phi_j = 2\pi j/n$, $j = 1, 2, \dots, n$.

5.3. Approximating the Vorob'ev expectation. To compute the Vorob'ev expectation, we have to perform two different tasks: At first, we have to approximate the coverage function p and afterwards, we have to compute the level value μ . In order to address these tasks, we refer to [19], where in particular the convergence of the subsequent estimators to p and $\mathbb{E}[\mathcal{L}(D)]$ is proven.

The idea is to build an estimator for the coverage function p by the empirical mean

$$p(\mathbf{x}) = \int_{\square} \mathbf{1}_{D(\mathbf{y})}(\mathbf{x}) \rho(\mathbf{y}) \, d\mathbf{y} \approx p_M(\mathbf{x}) := \frac{1}{M} \sum_{i=1}^M \mathbf{1}_{D(\mathbf{y}_i)}(\mathbf{x}) \rho(\mathbf{y}_i).$$

We compute the approximate coverage function on the circular grid¹

$$(5.17) \quad \mathbf{x}_{k,\ell} = \left(\frac{k}{n} R \cos \left(\frac{2\pi\ell}{n} \right), \frac{k}{n} R \sin \left(\frac{2\pi\ell}{n} \right) \right), \quad k, \ell = \{0, 1, \dots, n-1\}.$$

Here, the radius R has to be chosen such that $p(\mathbf{x}) = 0$ for all $\|\mathbf{x}\| \geq R$ which is possible due to Theorem 2.4. Consequently, the empirical volume

$$\text{Vol} = \int_{\mathbb{R}^2} p(\mathbf{x}) \, d\mathbf{x} = \int_0^{2\pi} \int_0^R p(r, \phi) r \, dr d\phi$$

¹A rectangular grid can of course be considered as well.

can be approximated by means of a trapezoidal rules in accordance with²

$$\text{Vol}_M := \frac{2\pi R}{n^2} \sum_{k,\ell=0}^{n-1} k p_M(\mathbf{x}_{k,\ell}).$$

The computation of μ amounts to the solution of the equation

$$(5.18) \quad \mathcal{L}(\{p > \mu\}) \leq \text{Vol}_M \leq \mathcal{L}(\{p \geq \mu\}).$$

Notice that the function $\Phi: \mu \mapsto \mathcal{L}(\{p \geq \mu\})$ is strictly decreasing on $[0, 1]$ since the level sets $\{p \geq \mu\}$ are nested. Therefore, the former equation has at most one solution. The question of existence is related to the continuity of the function Φ that is a priori only right continuous with left limits. Nevertheless, as a decreasing function, Φ jumps only on a countable subset of $[0, 1]$. In order to solve (5.18), we will use a simple bisection method.

5.4. Computing domain integrals. In order to evaluate the Vorob'ev expectation and also Vorob'ev deviation, we have to be able to approximate domain integrals of the form

$$(5.19) \quad I(L) := \int_L f(\mathbf{x}) \, d\mathbf{x}.$$

Here, L is a given domain which in our application coincides with the level set $\{p \geq \mu\}$ is a given level set (which is assumed to have a sufficiently smooth boundary). Moreover, the integrand f is assumed to be at least continuous. The numerical computation of the integral (5.19) is then performed by triangulating the set L with a mesh of width $h \approx 1/n$. To that end, we denote by $Q_{k,\ell}$ the grid cell, which is induced by the grid (5.17) and described the vertices $\mathbf{x}_{k,\ell}$, $\mathbf{x}_{k+1,\ell}$, $\mathbf{x}_{k,\ell+1}$, and $\mathbf{x}_{k+1,\ell+1}$. A grid cell can either lie inside L or it can lie outside L or it can intersect with the boundary of L . To determine which situation applies, we check if the approximate values of $p(\mathbf{x}_{k,\ell})$, $p(\mathbf{x}_{k+1,\ell})$, $p(\mathbf{x}_{k,\ell+1})$, and $p(\mathbf{x}_{k+1,\ell+1})$ are less or greater than μ . When a grid cell contains vertices which are less and greater than μ , we can determine a polygonal approximation to the boundary ∂L of the level set L by bilinear interpolation. The enclosed polygonal domain will be denoted by L_n .

Next, we subdivide grid cells that intersect the boundary ∂L_n into suitable triangles. In the remaining part of L_n , we subdivide each grid cell into two triangles. Figure 5.4 exemplifies a triangulation produced by our algorithm.

Having this triangulation at hand, we can easily apply a quadrature formula for triangles in order to approximate the integral (5.19).

²We implicitly used here that $p(\mathbf{0}) = 0$ which holds due to the fact that the origin is always enclosed by the interior boundary due to $q(\phi, \mathbf{y}) > 0$ for all $\phi \in I$ and $\mathbf{y} \in \square$.

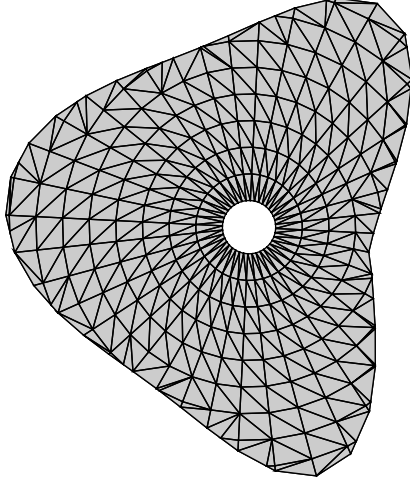


FIGURE 5.4. Triangulation of a kite shaped domain with circular hole.

Theorem 5.1. *Assume that $L \in C^2$ and $f \in C^2(\overline{L \cup L_n})$. Then, the above quadrature algorithm computes the integral $I(L)$ from (5.19) with accuracy $\mathcal{O}(h^2)$ provided that the element quadrature formulae are exact for linear polynomials.*

Proof. We shall first estimate the error which is induced by approximating the domain. Since ∂L_n is a piecewise linear approximation of step size h to the boundary curve ∂L , the area $|L \cap Q_{k,\ell}|$ of each quadrilateral $Q_{k,\ell}$ for which $Q_{k,\ell} \cap \partial L \neq \emptyset$ is approximated of order

$$||L \cap Q_{k,\ell}| - |L_n \cap Q_{k,\ell}|| = \mathcal{O}(h^3).$$

Taking into account that there are at most $\mathcal{O}(n)$ quadrilaterals that intersect the boundary curve, we conclude

$$(5.20) \quad |I(L) - I(L_n)| = \mathcal{O}(h^2).$$

Next, we estimate the error of quadrature on the polygonal domain L_n . The triangulation of L_n consists $\mathcal{O}(n^2)$ elements of volume $\mathcal{O}(h^2)$. Consequently, since the element quadrature formulae are exact of order two, we get an error of quadrature $\mathcal{O}(h^4)$ per element. Thus, denoting the result of the composite quadrature formula by $Q(D_n)$, we conclude

$$(5.21) \quad |I(D_n) - Q(D_n)| = \mathcal{O}(h^2).$$

By combining both estimates (5.20) and (5.21), we obtain the assertion due to

$$|I(D) - Q(D_n)| \leq |I(D) - I(D_n)| + |I(D_n) - Q(D_n)|.$$

□

Remark 5.2. *In three dimensions, one introduces a triangulation of the free surface and, henceforth, a tetrahedral mesh of the domain. As one readily verifies by following the above arguments, the same error estimate holds. Nevertheless, the complexity of the algorithm is $\mathcal{O}(h^{-3})$ instead $\mathcal{O}(h^{-2})$.*

6. NUMERICAL RESULTS

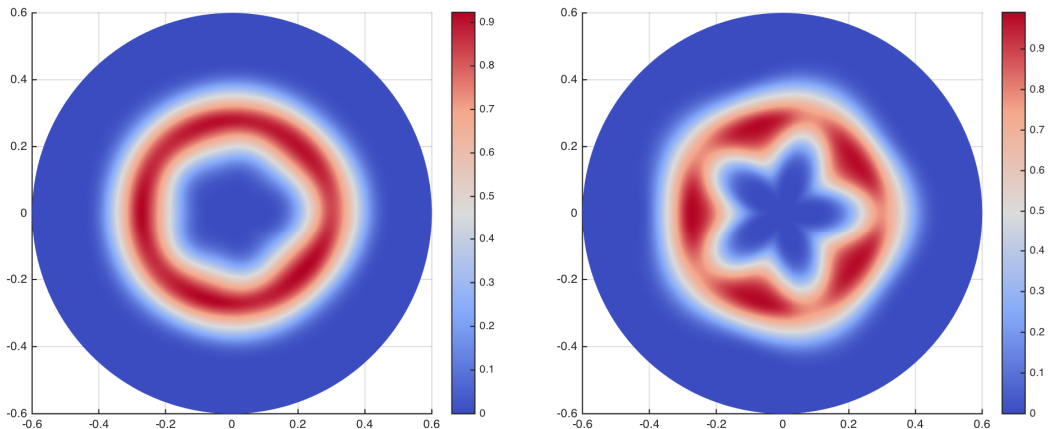


FIGURE 6.5. Coverage functions for the first example (left) and the second example (right).

In this section, we provide two numerical examples in order to illustrate our approach. For the numerical solution of the free boundary problem for each instance of the random parameter $\omega \in \Omega$, we apply the trial method which has been proposed in the preceding section. The iteration is stopped if the ℓ^∞ -norm of the update becomes smaller than 10^{-7} . For the discretization of the free boundary, we employ a trigonometric polynomial of order 32, i.e., $p = 16$ in (4.11). For the Nyström method, we use $n = 1024$ collocation points.

6.1. First example. In our first example, we consider the approximation of the expectation and the deviation of the solution to (1.2) in case of a randomly perturbed potatoe shaped inner domain. For the data, we prescribe the boundary conditions $u(\omega) = 1$ on $\Sigma(\omega)$ and $\|\nabla u(\omega)\|_2 = 6$ on $\Gamma(\omega)$. The radial function for $\Sigma(\omega)$ is given by

$$(6.22) \quad q(\phi, \omega) = 0.2 + 0.01f(\phi) + \sum_{k=1}^{10} \frac{\sqrt{2}}{k} \{ \sin(k\phi)X_{2k-1}(\omega) + \cos(k\phi)X_{2k}(\omega) \},$$

where $f(\phi)$ is a trigonometric polynomial with coefficients, cf. (4.11),

$$[a_6, \dots, a_0, b_1, \dots, b_5] = [0, 0.76, 0.26, 0.51, 0.70, 0.89, 0.96, 0.55, 0.14, 0.15, 0.26, 0].$$

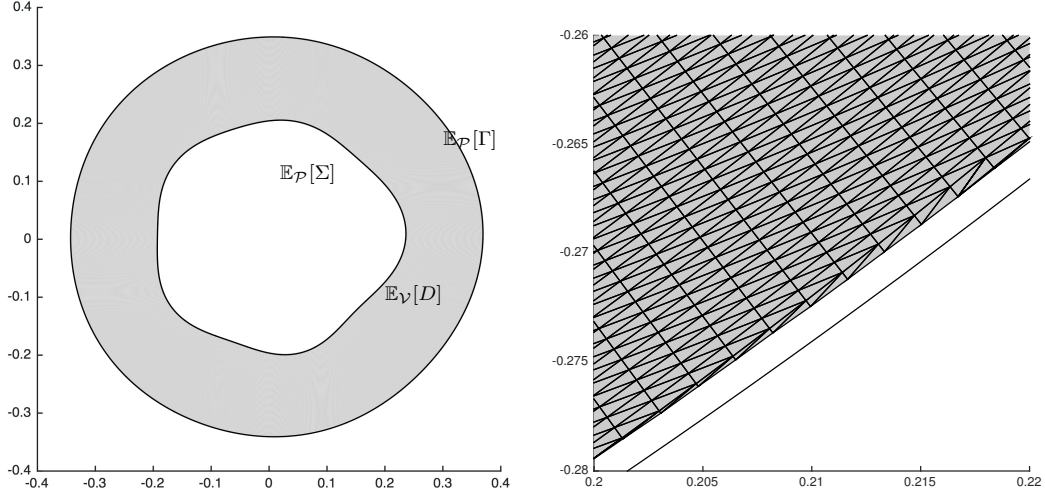


FIGURE 6.6. The expected domain (left) and a magnification of the area $[0.2, 0.22] \times [-0.28, -0.26]$ (right) for the first example.

The random variables $\{X_k\}_k$ are chosen to be independent and uniformly distributed in $[-1, 1]$. The approximation of the parametric expectations $\mathbb{E}_{\mathcal{P}}[\Sigma]$ and $\mathbb{E}_{\mathcal{P}}[\Gamma]$ as well as the computation of the domain's probability density p is performed by the application of a quasi-Monte Carlo quadrature based on 10^5 Halton points, cf. [14]. On the left hand side of Figure 6.6, we have depicted the corresponding curves for $\mathbb{E}_{\mathcal{P}}[\Sigma]$ and $\mathbb{E}_{\mathcal{P}}[\Gamma]$ in black. The grey-shaded area indicates the Vorob'ev expectation $\mathbb{E}_{\mathcal{V}}[D]$. The latter is computed via the sampled probability density, which is depicted on the left hand side of Figure 6.5. As one can clearly see from the visualization, there is nearly no difference between the Vorob'ev expectation $\mathbb{E}_{\mathcal{V}}[D]$ and the parametric expectation $\mathbb{E}_{\mathcal{P}}[D]$. Still, as can be seen from the magnification on the right hand side of Figure 6.6, there is actually a difference. The corresponding deviations are listed in Table 6.1.

$\mathcal{D}_{\mathcal{P}}[\Sigma]$	$\mathcal{D}_{\mathcal{P}}[\Gamma]$	$\mathcal{D}_{\mathcal{V}}[D]$
0.106323591117	0.0756434104	0.1306199403

TABLE 6.1. Deviations for the first example.

6.2. Second example. For our second example, we choose a model that is similar to (6.22), but with another expected shape, which is given by the trigonometric polynomial with coefficients

$$[a_6, \dots, a_0, b_1, \dots, b_5] = [0, 4, 0, 0, 0, 0, 0, 0, 0, 0, 0, 0].$$

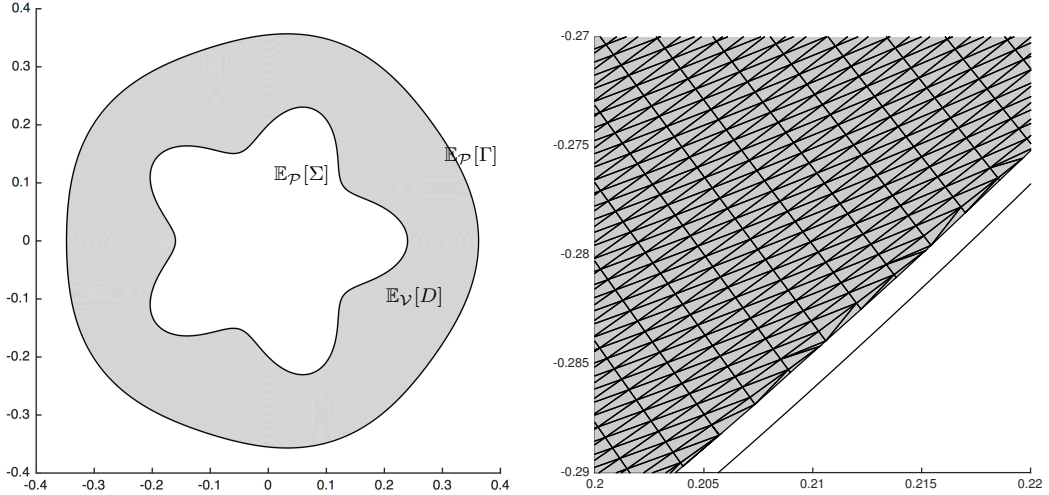


FIGURE 6.7. The expected domain (left) and a magnification of the area $[0.2, 0.22] \times [-0.29, -0.27]$ (right) for the second example.

All other parameters are kept as before. This means that the two examples only differ in the chosen expectation for the interior domain. The different notions of expectations for this example can be found on the left hand side of Figure 6.7. Again, there is nearly no difference between the Vorob'ev expectation and the domain which is enclosed by the parametric expectations $\mathbb{E}_{\mathcal{P}}[\Sigma]$ and $\mathbb{E}_{\mathcal{P}}[\Gamma]$. On the right hand side of the same figure, we have also depicted a magnification. The corresponding coverage function is found on the right hand side of Figure 6.5. As can be inferred from Table 6.2, the parametric deviation $\mathcal{D}_{\mathcal{P}}[\Sigma]$ coincides with that from the previous example, cf. Table 6.1. This can be explained due to the fact that we chose the same underlying model up to the different expected shapes of the inclusion. The difference in $\mathcal{D}_{\mathcal{P}}[\Gamma]$ between the two examples is rather small, too. The same observation holds also with respect to the Vorob'ev deviation.

$\mathcal{D}_{\mathcal{P}}[\Sigma]$	$\mathcal{D}_{\mathcal{P}}[\Gamma]$	$\mathcal{D}_{\mathcal{V}}[D]$
0.106323591117	0.0772838425	0.1297053208

TABLE 6.2. Deviations for the second example.

7. CONCLUSION

In this article, we have dealt with Bernoulli's exterior free boundary problem in the situation of an interior boundary which is random. Such uncertainties may arise from tolerances in fabrication processes or from measurement errors. If the interior

boundaries are star-shaped, then the problem under consideration can be shown to be well-posed. We have presented two different notions of the expectation and the deviation of the resulting annular domain. Indeed, we have proven that these two definitions are actually distinct from each other. Still, our numerical examples indicate that there may only be a very small difference in practice.

REFERENCES

- [1] A. Acker. On the geometric form of Bernoulli configurations. *Mathematical Methods in the Applied Sciences*, 10(1):1–14, 1988.
- [2] A. Acker and R. Meyer. A free boundary problem for the p -laplacian: uniqueness, convexity, and successive approximation of solutions. *Electronic Journal of Differential Equations*, 8:1–20, 1995.
- [3] H. W. Alt and L. A. Caffarelli. Existence and regularity for a minimum problem with free boundary. *Journal für die reine und angewandte Mathematik*, 325:105–144, 1981.
- [4] A. Beurling. On free boundary problems for the Laplace equation. *Seminars on Analytic functions, Institute for Advanced Study, Princeton, NJ*, 1:248–263, 1957.
- [5] F. Bouchon, S. Clain, and R. Touzani. Numerical solution of the free boundary Bernoulli problem using a level set formulation. *Comput. Methods Appl. Mech. Engrg.*, 194(36-38):3934–3948, 2005.
- [6] M. Bugeanu and H. Harbrecht. A second order convergent trial method for a free boundary problem in three dimensions. *Interfaces Free Bound.*, 17(4):517–537, 2015.
- [7] R. Caffisch. Monte Carlo and quasi-Monte Carlo methods. *Acta Numerica*, 7:1–49, 1998.
- [8] C. Chevalier, D. Ginsbourger, J. Bect, and I. Molchanov. Estimating and quantifying uncertainties on level sets using the Vorob’ev expectation and deviation with gaussian process models. In Dariusz Ucinski, Anthony C. Atkinson, and Maciej Patan, editors, *mODa 10 – Advances in Model-Oriented Design and Analysis: Proceedings of the 10th International Workshop in Model-Oriented Design and Analysis Held in Lagów Lubuski, Poland, June 10–14, 2013*, pages 35–43, Heidelberg, 2013. Springer International Publishing.
- [9] M. Crouzeix. Variational approach of a magnetic shaping problem. *European Journal of Mechanics B-Fluids*, 10:527–536, 1991.
- [10] J. Descloux. Stability of the solutions of the bidimensional magnetic shaping problem in absence of surface tension. *European Journal of Mechanics B-Fluids*, 10:513–526, 1991.
- [11] K. Eppler and H. Harbrecht. Efficient treatment of stationary free boundary problems. *Appl. Numer. Math.*, 56(10-11):1326–1339, 2006.
- [12] M. Flucher and M. Rumpf. Bernoulli’s free-boundary problem, qualitative theory and numerical approximation. *Journal für die reine und angewandte Mathematik*, 486:165–204, 1997.

- [13] A. Friedman. Free boundary problem in fluid dynamics. *Astérisque*, 118:55–67, 1984.
- [14] J. H. Halton. On the efficiency of certain quasi-random sequences of points in evaluating multi-dimensional integrals. *Numerische Mathematik*, 2(1):84–90, 1960.
- [15] H. Harbrecht and G. Mitrou. Improved trial methods for a class of generalized Bernoulli problems. *Journal of Mathematical Analysis and Applications*, 420(1):177 – 194, 2014.
- [16] H. Harbrecht and M. Peters. Solution of free boundary problems in the presence of geometric uncertainties. *Preprint 2015-02 Mathematisches Institut Universität Basel*, 2015. to appear in Radon Series on Computational and Applied Mathematics, de Gruyter.
- [17] H. Harbrecht, M. Peters, and M. Siebenmorgen. Efficient approximation of random fields for numerical applications. *Numerical Linear Algebra with Applications*, 2015. to appear.
- [18] J. Haslinger, T. Kozubek, K. Kunisch, and G. Peichl. Shape optimization and fictitious domain approach for solving free boundary problems of Bernoulli type. *Comput. Optim. Appl.*, 26(3):231–251, 2003.
- [19] P. Heinrich, R. S. Stoica, and V. C. Tran. Level sets estimation and vorob'ev expectation of random compact sets. *Spatial Statistics*, 2(1):47–61, 2012.
- [20] E. Hille and R. S. Phillips. *Functional analysis and semi-groups*, volume 31. American Mathematical Society, Providence, 1957.
- [21] K. Ito, K. Kunisch, and G. H. Peichl. Variational approach to shape derivatives for a class of Bernoulli problems. *J. Math. Anal. Appl.*, 314(1):126–149, 2006.
- [22] R. Kress. *Linear integral equations*. Vol. 82 of Applied Mathematical Sciences. Springer, New York, 2nd edition, 1999.
- [23] M. Loève. *Probability theory. I+II*. Number 45 in Graduate Texts in Mathematics. Springer, New York, 4th edition, 1977.
- [24] I. Molchanov. *Theory of random sets*. Probability and its Applications (New York). Springer-Verlag London, Ltd., London, 2005.
- [25] D. E. Tepper. On a free boundary problem, the starlike case. *SIAM Journal on Mathematical Analysis*, 6(3):503–505, 1975.
- [26] T. Tiihonen. Shape optimization and trial methods for free boundary problems. *RAIRO Modél. Math. Anal. Numér.*, 31(7):805–825, 1997.
- [27] T. Tiihonen and J. Järvinen. On fixed point (trial) methods for free boundary problems. In S.N. Antontsev, A.M. Khludnev, and K.-H. Hoffmann, editors, *Free Boundary Problems in Continuum Mechanics*, volume 106 of *International Series of Numerical Mathematics*, pages 339–350. Birkäuser, Basel, 1992.

MARC DAMBRINE, UNIVERSITÉ DE PAU ET DES PAYS DE L'ADOUR, IPRA-LMA, UMR
CNRS 5142 AVENUE DE L'UNIVERSITÉ, 64000 PAU, FRANCE

E-mail address: `marc.dambrine@univ-pau.fr`

HELMUT HARBRECHT, UNIVERSITÄT BASEL, DEPARTEMENT MATHEMATIK UND INFOR-
MATIK, SPIEGELGASSE 1, 4051 BASEL, SCHWEIZ

E-mail address: `helmut.harbrecht@unibas.ch`

MICHAEL D. PETERS, UNIVERSITÄT BASEL, DEPARTEMENT MATHEMATIK UND INFOR-
MATIK, SPIEGELGASSE 1, 4051 BASEL, SCHWEIZ

E-mail address: `michael.peters@unibas.ch`

BÉNÉDICTE PUIG, UNIVERSITÉ DE PAU ET DES PAYS DE L'ADOUR, IPRA-LMA, UMR
CNRS 5142 AVENUE DE L'UNIVERSITÉ, 64000 PAU, FRANCE

E-mail address: `bpuig@univ-pau.fr`

LATEST PREPRINTS

- No.** **Author:** *Title*
- 2016-06 **M. Dambrine, I. Greff, H. Harbrecht, B. Puig**
Numerical solution of the homogeneous Neumann boundary value problem on domains with a thin layer of random thickness
- 2016-07 **G. Alberti, G. Crippa, A. L. Mazzucato**
Exponential self-similar mixing by incompressible flows
- 2016-08 **M. Bainbridge, P. Habegger, M. Möller**
Teichmüller curves in genus three and just likely intersections in $G_m^n \times G_a^n$
- 2016-09 **Gabriel A. Dill**
Effective approximation and Diophantine applications
- 2016-10 **J. Blanc, S. Zimmermann**
Topological simplicity of the Cremona groups
- 2016-11 **I. Hedén, S. Zimmermann**
The decomposition group of a line in the plane
- 2016-12 **J. Ballani, D. Kressner, M. Peters**
Multilevel tensor approximation of PDEs with random data
- 2016-13 **M. J. Grote, M. Kray, U. Nahum**
Adaptive eigenspace method for inverse scattering problems in the frequency domain
- 2016-14 **H. Harbrecht, M. Peters, M. Schmidlin**
Uncertainty quantification for PDEs with anisotropic random diffusion
- 2016-15 **F. Da Lio, L. Martinazzi**
The nonlocal Liouville-type equation in R and conformal immersions of the disk with boundary singularities
- 2016-16 **A. Hyder**
Conformally Euclidean metrics on R^n with arbitrary total Q -curvature
- 2016-17 **G. Mancini, L. Martinazzi**
The Moser-Trudinger inequality and its extremals on a disk via energy estimates
- 2016-18 **R. N. Gantner, M. D. Peters**
Higher order quasi-Monte Carlo for Bayesian shape inversion

LATEST PREPRINTS

No.	Author: Title
2016-19	C. Urech <i>Remarks on the degree growth of birational transformations</i>
2016-20	S. Dahlke, H. Harbrecht, M. Utzinger, M. Weimar <i>Adaptive wavelet BEM for boundary integral equations: Theory and numerical experiments</i>
2016-21	A. Hyder, S. Iula, L. Martinazzi <i>Large blow-up sets for the prescribed Q-curvature equation in the Euclidean space</i>
2016-22	P. Habegger <i>The norm of Gaussian periods</i>
2016-23	P. Habegger <i>Diophantine approximations on definable sets</i>
2016-24	F. Amoroso, D. Masser <i>Lower bounds for the height in Galois extensions</i>
2016-25	W. D. Brownawell, D. W. Masser <i>Zero estimates with moving targets</i>
2016-26	H. Derksen, D. Masser <i>Linear equations over multiplicative groups, recurrences, and mixing III</i>
2016-27	D. Bertrand, D. Masser, A. Pillay, U. Zannier <i>Relative Manin-Mumford for semi-abelian surfaces</i>
2016-28	L. Capuano, D. Masser, J. Pila, U. Zannier <i>Rational points on Grassmannians and unlikely intersections in tori</i>
2016-29	C. Nobili, F. Otto <i>Limitations of the background field method applied to Rayleigh-Bénard convection</i>
2016-30	W. D. Brownawell, D. W. Masser <i>Unlikely intersections for curves in additive groups over positive characteristic</i>
2016-31	M. Dambrine, H. Harbrecht, M. D. Peters, B. Puig <i>On Bernoulli's free boundary problem with a random boundary</i>